2. LONGITUDINAL DYNAMICS OF RAILWAY BOGIES: A LITERATURE REVIEW

2.1. INTRODUCTION

Railway bogies are often subjected to longitudinal forces due to a number of train related dynamics including braking and traction. These longitudinal forces affect the dynamics of bogies in a complex manner. Severe braking or traction may affect the safety and stability of bogies adversely. Thus, there is a need to study the bogie dynamics as a function of the longitudinal forces with a view to minimising the risk to railway transportation.

For the proper analysis of the dynamic performance of bogies under braking or traction, basic understanding of the vertical and lateral dynamics of the wagon is required. The first part of this chapter introduces some important terms that relate to the dynamics of wagons. The mechanics of wheel-rail contact, which is fundamental to the bogie and wagon dynamics, is also discussed in this chapter. The wagon braking and traction systems and their principle of working are reviewed briefly for completeness. In the last part of this chapter, a review of the current railway wagon simulation software systems and their limitation to perform wagon longitudinal dynamics simulation is presented.

2.1.1. Basic Axis System and Terminologies

To discuss the dynamics of the wagon a coordinate system containing six degrees of freedom as shown in Fig 2.1 is normally used. Linear motion along the X, Y and Z axes are termed as longitudinal, lateral, and vertical translations respectively.

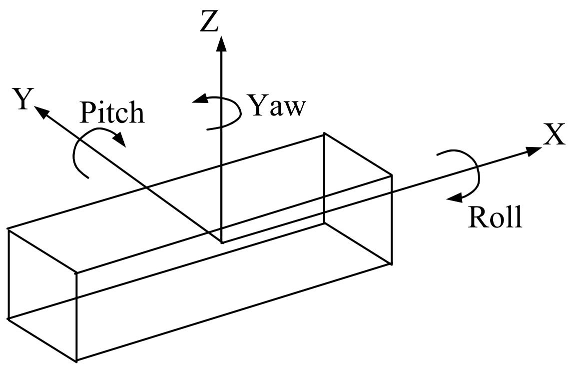

Figure 2.1. Six degrees of freedom of wagon movement

The rotations are defined in accordance to the right hand screw rule where the positive rotation is seen as clockwise if the observer is stationed at the origin and looks at the axes in the positive direction. Rotary motions about the X, Y and Z axes are termed as roll, pitch and yaw respectively (see Fig.2.1).

2.1.2. Wagon Assembly and Tracks Construction

Wagon components and assembly

Most wagons that are currently in use consist of a body and two bogies that provide the necessary suspension. Each bogie basically consists of two wheelsets, a bogie frame consisting of two side frames and one bolster, as well as spring nests. A few commonly available bogies are exhibited in Fig.2.2 - 2.4.

Two common types of bogies widely used in freight trains are three-piece bogies and Y25 bogies. The first is widely used in the United States, Australia, and Asia while the second in Europe (Harder (2000), Bosso et al. (2000)). Fig.2.2 shows a typical three-piece bogie and Fig.2.3 shows a typical Y25 bogie.

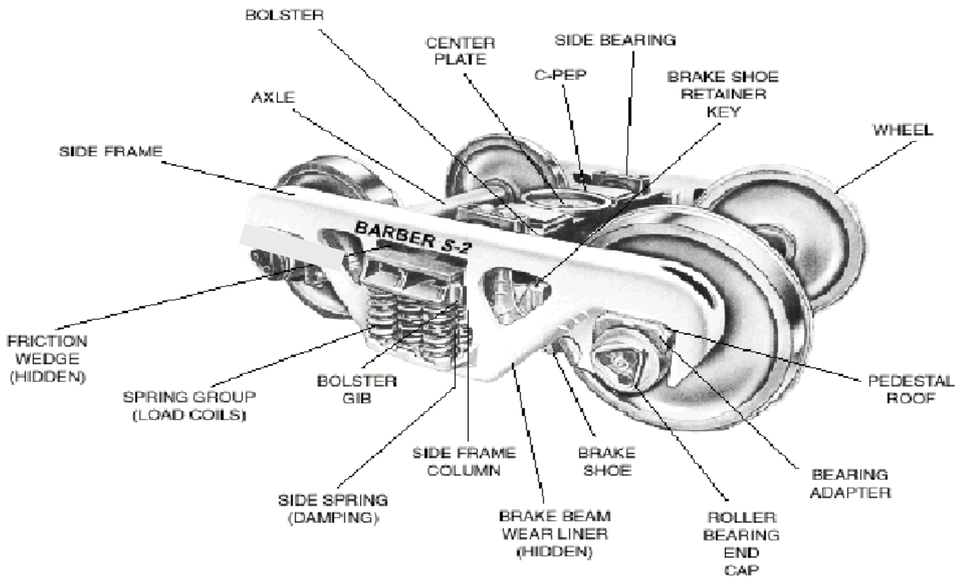

Figure 2.2. Typical design of three-piece bogie (Company Standard Car Truck (2000))

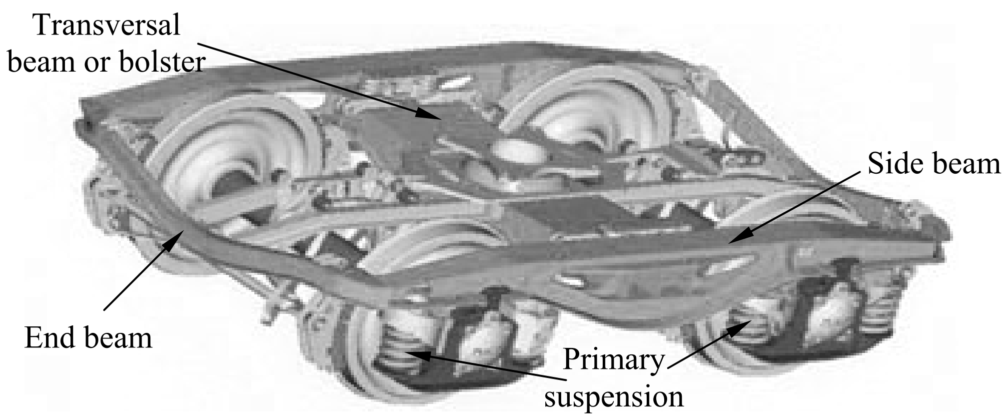

Figure 2.3. Typical design of Y25 bogie (Website K. Industrier. AB (2005))

Three-piece bogies consist of a bolster, two side frames and two wheelsets. This type of bogie does not have primary suspension while the secondary suspension is made from coil springs that connect the bolster with the side frame. Damping is provided by friction wedges, which are placed between the side frame and the bolster.

In contrast to the three-piece bogies, Y25 bogies do not have secondary suspension. They have only primary suspensions that connect the wheelsets and the side frame. The primary suspensions are formed from coil springs and *Lenoir links* which provide friction damping. The bogie frame is constructed from two side beams, one transverse beam or bolster and two end beams.

The three-piece bogies and the Y25 bogies are very popular as they are cheap to purchase and maintain. However, their simple design leads to low levels of lateral stability and ride quality, and higher levels of track forces due to vertical and lateral impacts as well as the angle of attack in curved tracks (Stichel (1999)). Although the performance of both bogies fulfils most of the requirements for freight wagon operations, in some cases a higher performance bogie will be needed. In such cases, at the expense of initial cost, bogies containing both primary and secondary suspensions are used. An example of this type of bogie is shown in Fig 2.4.

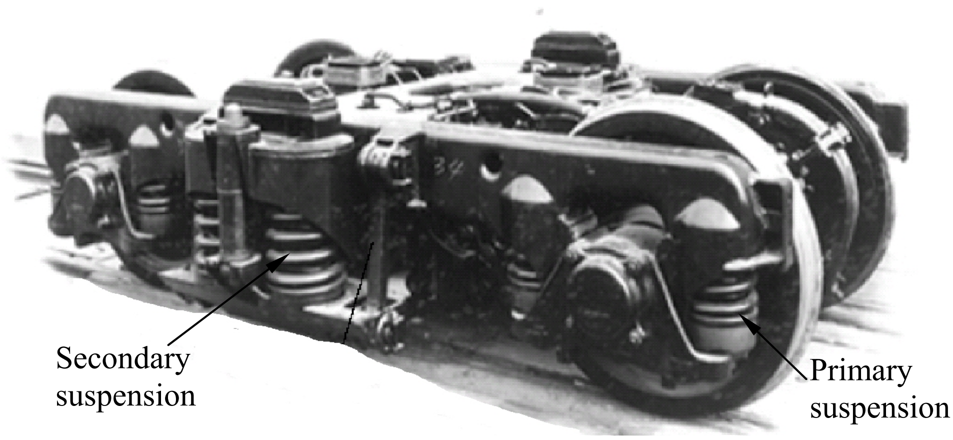

Figure 2.4. Bogie with primary and secondary suspension (Ikamoto (1998))

Track construction

Track is one of the most important technical elements required for the railway operation. Its main function is to provide guidance for the wagons in addition to supporting the heavy mass of the running train and absorbing the induced vibration. Track possesses a complex structure with elastic and dissipative properties. Fig. 2.5 (Profilidis (2000)) exhibits the basic construction of a traditional railway track that consists of a pair of rails, sleepers and track support.

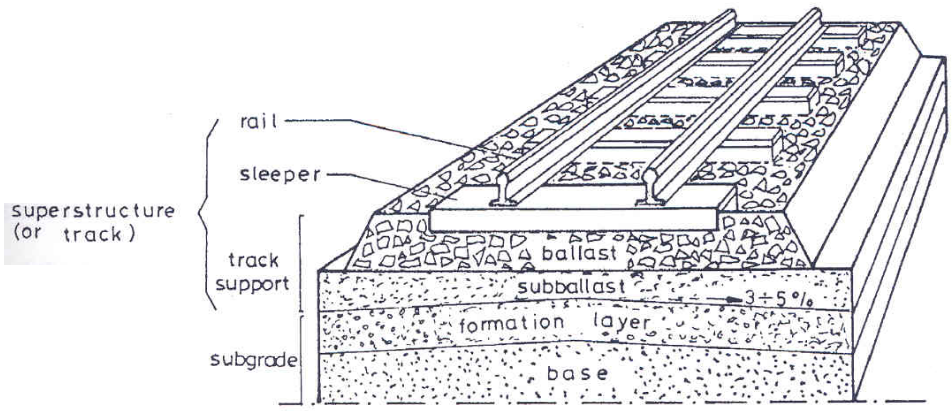

Figure 2.5. A Typical Track Structure (Profilidis (2000))

The requirements for the strength and quality of the track depend to a large extent on the following load parameters (Esveld (2001)):

- axle load: static vertical load per axle
- tonnage borne: sum of the axle loads
- dynamic and / or impact load

The static axle load level, to which the dynamic increment is added, in principle determines the required strength of the track. The dynamic load components, which depend on the operational speed and horizontal and vertical track geometry, are also essential factors in the track structure design.

2.2. DYNAMICS OF THE BOGIES

Train-track dynamics is largely due to the interaction between the complex geometries of the wheel and the rail within the contact patch that generates much high levels of contact forces. It also involves many degrees of freedom and forces that change rapidly and act at the same time at many points in the suspension system and couplers between wagons. The existence of track irregularities and wheel defects makes the problem more challenging to mathematically formulate. Hence an in depth understanding of the subject of the dynamics of multibody systems is essential.

2.2.1 Principles of Wheelset Dynamics

The dynamic characteristics of a railway bogie are defined by the interaction between the wheel and the rail, the configuration of suspensions and the articulation with adjacent wagons. Among these, the interaction between the wheel and the rail that characterises the dynamic behaviour of the railway wheelset running along the track is the most fundamental factor that affects the bogie dynamics.

The wheelset provides basic guidance of travel to railway bogies. The dynamics of a bogie is primarily affected by the dynamic behaviour of the wheelset and the track characteristics. Fig 2.6 depicts a railway wheelset positioned on the track. It could be seen that the conventional wheelset consisting of two conical wheels separated by a distance compatible to the gauge width of the track fixed to a common axle. This form has a long history and seems to have evolved by a process of trial and error (Wickens (1998)).

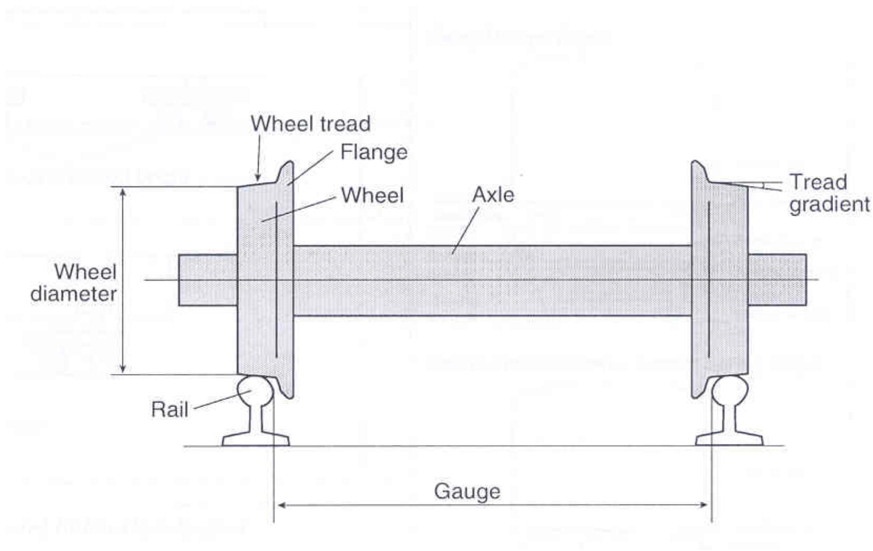

Figure 2.6. Wheelset on the track (Ikamoto (1998))

The observation of the dynamic behaviour of wheelsets has begun since the early years of the railway history. Marshal (1938) has reported that, not long after the conical wheel tread was established in 1821, George Stephenson in his *Observation on Edge and Tram Railway* had stated a very clear description of kinematic oscillation as shown in Fig.2.7. This kinematic oscillation could cause stability problem in the tangent track. The statement of George Stephenson can be found in Wickens (1998) and Wickens (2003).

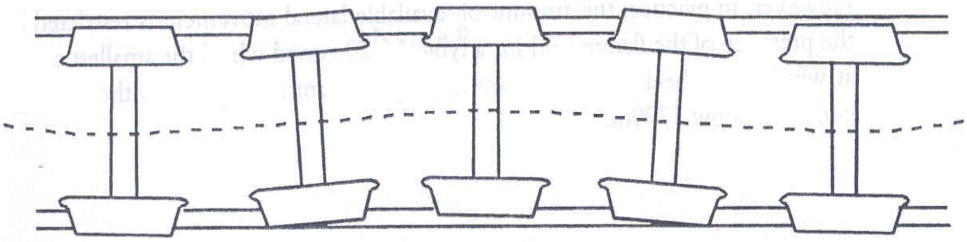

Figure 2.7. Wheelset Kinematic Oscillation (Wickens (2003))

Klingel (1883) formulated the first mathematical relationship for this kinematic oscillation and derived the relationship between the wavelength L_H and the wheelset conicity λ_w, nominal wheel radius r_w and lateral distance between the wheel-rail contact points $2l$ as shown in Eq.2.1.

$$L_H = 2\pi(\frac{r_w l}{\lambda_w})^{1/2} \qquad (2.1)$$

This simple formula is derived purely from the geometry analysis.

Although the conical wheel causes stability problems in the tangent track, it helps the wheelset to negotiate the curves with ease. A wheelset with conical wheels can maintain a pure rolling motion while running on a curve if it moves outward and takes the radial position. In his book, Wickens (2003) reported that Redtenbacher (1885) had performed a theoretical analysis to improve the understanding of the conical wheelset negotiating curves as illustrated in Fig.2.8.

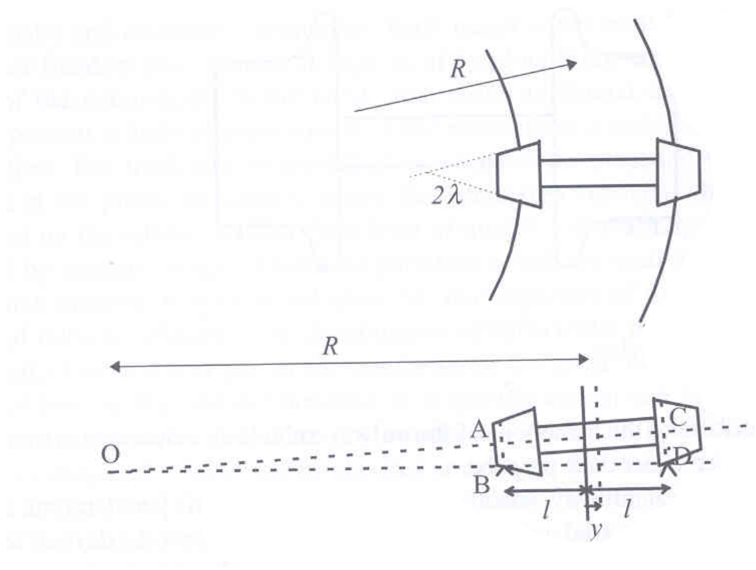

Figure 2.8. Conical wheelset on a curve (Wickens (2003))

From the geometry in Fig. 2.8 it can be seen that there is a simple relationship between the lateral movement of the wheelset y, the radius of curve R, the wheel radius r_w, the lateral distance between the points of contact of the wheels with the rails $2l$, and the conicity λ_w of the wheels in order to sustain pure rolling that is shown in Eq.2.2.

$$\begin{aligned} &OAB = OCD \\ &(r_w - \lambda_w y)/(R-l) = (r_w + \lambda_w y)/(R+l) \\ &y = r_w l / R\lambda_w \end{aligned} \tag{2.2}$$

As can be seen, the above two analyses of kinematic oscillation and curving are purely based on geometries of the wheel and the track. More detailed analysis of the dynamic behaviour of railway wheelset must be performed if the forces acting at the wheel-rail contact patch are desired.

2.2.2. State-of-the-art of the Study of Wagon and Bogie Dynamics

History and development

The revolution in the analysis of railway wagon dynamics started when the theory of creep (further discussed in Section 2.3) was first introduced by Carter (1926). With this theory, the wheel-rail contact forces can be determined and the equations of motion that describe the wheelset dynamics can also be derived.

Following the development of the creep theory that defines the interaction between the wheel and the rail, extensive studies of wagon dynamics were undertaken. In general the problem of wagon dynamics can be divided into two parts: the hunting or the stability problem which deals with the tangent track, and the curving behaviour which deals with curved track. Unfortunately there is a conflict between stability on the straight track and curving behaviour on the curved track. For example a softer and more flexible primary spring will give a better curving performance but it will reduce the lateral stability in the tangent track. Similarly harder springs will improve the lateral stability but lead to poor curving performance (defined by increase in angle of attack). Gilchrist (1998) has presented a good paper that reviews the history and the development of the research on the optimisation of the hunting and curving problems.

Matsudaira (1952) was the first to solve the complexity of the wheelset equation of motion and concluded that through proper design, a spring-restrained wheelset could be made stable up to any required critical speed as demonstrated by his theoretical work and experiments on a roller rig, where the stability was observed directly. Using his theory, he specified the suspension design parameters for the bogies of the first Shinkansen high speed train that was successfully introduced into service in 1964.

Following Matsudaira's work, from the mid fifties until the mid sixties most of the research on railway wagon dynamics were focused on the subject of stability. For example, de Pater (1956, 1961) investigated the non-linearity of the wheel-rail profile and its effect to wagon stability, and Wickens (1965-6) proved the importance of lateral damping of the primary suspension for the dynamic stability of the wheelset.

However, the more extensive study on wagon dynamics came after Kalker (1967), who studied the rolling contact between two elastic bodies, provided a theory that could be used to calculate forces generated in the wheel-rail rolling contact patch. The work of Kalker and the development in numerical techniques have widely opened the possibility of studying wagon dynamics through computer modelling to obtain better results. Since the pioneering work of Kalker, a large amount of research on wagon dynamics has been reported. It is impossible to present all of them in this review; a brief summary, however, is provided. The research covers the study on stability, curving performance, wagon-track dynamic interaction and control.

Hunting and stability

Rinehart (1978) has examined the hunting stability of three-axle locomotive bogies. Due to symmetry, he has simplified the system using an eleven DOF model representing a "half locomotive" (one bogie only). A set of laboratory test data of natural frequency and mode shapes was used to validate the model. The results showed that a hunting frequency of more than 4 Hz was obtained and the predicted hunting frequency from the mathematical model had good agreement with the measurement.

Tuten et al. (1979) investigated how various wheel profiles and asymmetric loading affected the stability of wagons. The investigation used a nine DOF wagon model. The results showed that the wagon stability strongly depended on the location of axles having different values of effective conicity and contact angles. The wheel profile mix of a particular bogie was shown to be of much greater importance than whether the bogie was put in the leading or trailing location. The asymmetric loading was also found to affect the lateral stability.

Renger (1984) modelled a railway vehicle with two-axle bogies to examine its lateral stability and ride quality. The vehicle response against the lateral centre line and the cross-level deviations of the track were evaluated. A few important results provided by the simulation are as follow:

(i) The stability and the riding quality could be improved by optimising the secondary lateral damping.

(ii) Instead of using the primary damping, the stability and lateral ride quality could be better improved through the optimisation of the primary stiffness.

De Pater (1989) studied the lateral stability of wagons containing two axle bogies. The study was purely analytical using a mathematical model. He showed that an appropriate choice of the lateral stiffness connecting the two wheelsets could increase the critical speed.

Ahmadian (1998) investigated the non-linear oscillation of the wheelset with flange contact. Bifurcation theory was applied to analyse the instability due to hunting. The studied case was a rail wheelset containing nonlinear primary yaw dampers. The result of the study showed that hunting could occur at speeds below the critical speed computed through a linear analysis due to nonlinearities caused by flange contact, gauge clearance and yaw dampers.

Yabuno et al. (2001) studied the stabilisation control for the hunting motion of the wheelsets. They proposed a control strategy to limit the hunting motion of the wheelsets. The control method focused on the asymmetry in the stiffness matrix that was the principal cause of hunting. In order to reduce the effect of the asymmetrical component of the matrix, a lateral force proportional to yaw motion was applied. An experimental study was also conducted to validate the theoretical result. It was concluded that the control strategy significantly increased the critical speed.

Mohan (2003) reported an investigation on the nonlinear analysis of the controllable primary suspensions to improve hunting stability of wagons through the use of various primary and secondary stiffness and damping parameters. It was concluded that the critical velocity of wagons was more sensitive to the primary longitudinal stiffness compared to other parameters. He also proposed a method to control hunting stability using semi-active control of the primary longitudinal stiffness.

Curving and derailment

Sweet et al. (1984) studied the running safety of wagons against wheel-climb derailment. The study employed theoretical modelling and experiments. The results showed that the derailment quotient or the ratio of the lateral to the vertical force (L/V ratio) at the wheel-rail interface alone was not sufficient to predict the safety against derailment. Under dynamic conditions, a significantly larger derailment quotient could occur without causing actual derailment if it only occurred for a very short time. Hence the criterion for derailment was accounted for by both the derailment quotient and the corresponding duration.

Effects of wheel-rail contact geometry to the wheelset steering forces was studied by Mace et al. (1996). The study involved both field experiments and theoretical analysis. It was reported that the hollow worn wheel adversely affected the wheelset steering during negotiating curves, leading to the generation of large negative steering moments. These negative steering moments caused a number of undesirable effects such as the track gauge widening, the rail roll over, the extensive wear of the wheel and the rail, and the increased train rolling resistance.

Haque et al. (1996) reported a non-linear wheelset model for derailment prediction. The modelling provided special emphasis on safety-related behaviour of the wheelset negotiating both the tangent and curved tracks. The wheelset models accounted for non-linearities due to wheel-rail profile geometry and creep force and the longitudinal translation of the contact patch as a function of wheelset yaw angle. The wheelset model was claimed to have lateral, yaw, and spin degrees of freedom and considered single-point and two-point contact as well as transition from one to the other. The authors exhibited that the model was capable of predicting the wheelset dynamic behaviour during wheel climb, wheel lift, steering characteristics during curve negotiation and also limit cycle behaviour on the tangent track.

Nagase et al. (2002) reported experimental results of the wheel climb derailment. The experiment was performed using a model bogie and a model track (1:5 scale). The risk of the derailment was evaluated using Nadal formula (ratio of the lateral force to the vertical force applied to the wheel) as well as by measuring the wheel vertical displacement using a high-precision laser displacement sensor. As a result, it was found that the adhesion coefficient had a major influence on the occurrence of wheel climb derailment.

Optimisation of hunting and curving behaviour

Wickens (1991) provided a detailed review on optimisation of the hunting and curving behaviour through suspension design using sophisticated mathematical modelling. Current suspension technology has opened possibilities to develop innovative bogie designs with optimal performance in both tangent and curved tracks.

Matsumoto et al. (1999) proposed some methods to optimise the curving behaviour without reducing the hunting speed of the wagon. These methods included optimised worn tread profiles of wheels, independently rotating wheels in the rear axle, and asymmetric arrangement of the longitudinal primary suspension. The third method had earlier been proposed by Suda and Anderson (1994).

The improvement of the compatibility of the lateral stability and the curving performance of a railway passenger bogie was recently reported by Dukkipati and Narayanaswamy (2004). The authors proposed that the stiffness of the primary suspension of the leading axle be set different to the trailing axle.

Wagon and track interaction

All of the above reported research works have been focusing on the study of wagon and/or bogie dynamics without providing much attention to the track structure by assuming the track as a rigid or a simple elastic support. There are several studies, on the other hand, that focus only on the railway track dynamics by simplification of input disturbance from the measurement or pre-calculated wagon dynamic characteristics (Grassie (1992), Luo et al. (1996), and Kerr (2000)). Some other studies on track dynamics have considered the track and the wagon as a multi-body system but simplified the case to only the vertical interaction between the wagon and the track (Zhai and Sun (1993)and Ripke and Knothe (1995)).

However, sometimes it is necessary to fully describe both the wagon and the track structures in 3D to examine their interaction with each other in all directions. This is because the track structure can affect the wheel rail interaction forces that play an important role in determining the dynamic behaviour of wagons. On the other hand, wagon suspension design can also affect the forces imposed on the track.

Sun and Dhanasekar (2001) introduced a three dimensional wagon track system dynamics (3D-WTSD) model, which fully describes the dynamic behaviour of the wagon and the track when the wagon runs under constant speed on tangent tracks. The 3D-WTSD model can be used, for example, to investigate the effect of track design parameters both on the wagon and the track dynamics or vice versa to investigate the effect of suspension design parameters on both the wagon and the track dynamics. It also can be an effective tool to investigate the effect of track on wagon dynamics and the effect of lateral and vertical impact applied by the wagon to track dynamics (Sun (2002)). From the results of simulations using 3D-WTSD model, Sun and Dhanasekar (2004) also reported the importance of track modelling for the determination of the critical speed of wagons. A similar example of the simulation that takes into account the 3D dynamic behaviour of the wagon and the track was presented by Anderson and Abrahamsson (2002).

In the case of wagon dynamics under traction/braking condition, the vertical and the lateral impact forces applied to the track may not be an issue. However, when the traction/braking force is applied to the wheels a large longitudinal creep force arises in the wheel-rail contact area. This force will dissipate through the structure below the rail such as the sleepers and the ballast. If this longitudinal force is big enough, the sleepers can be displaced from their position. If a train is braked or accelerated on the construction such as the railway bridge, the longitudinal force generated will be also passed through the construction. Therefore, in designing the track structure and the railway bridge this longitudinal force is required to be accounted for.

All of the above described simulation models deal with only *constant speed* without any reference to deceleration or acceleration. The dynamics of wagons under braking/traction is reviewed in Section 2.5.

2.3. THEORY OF WHEEL-RAIL ROLLING CONTACT

This section briefly reviews the development of wheel-rail rolling contact theory, which forms the foundation for determining the wheel-rail interaction forces. The accurate calculation of the wheel-rail interaction forces is very important in the modelling of the railway wagon and bogie dynamics. Kalker (1991) has provided a very good presentation on this subject. Another good reference is a book by Garg and Dukkipati (1984). Details of the mathematical analysis on rolling contact phenomena can be found in Jacobson and Kalker (2000) and Kalker (1990).

2.3.1. The Concept of Creep

Consider two rigid bodies that are in contact at a point. If any one or both of these bodies are rotated and/or moved relative to each other, the contact point will also shift its original position; the resulting velocities of the contact point over each body might or might not be equal to each other. When the velocities are equal, the bodies are said to be undergoing *pure rolling* (with no creep); under unequal velocities, they are said to be undergoing *rolling coupled with sliding (i.e., with creep). Creep* or *creepage* is a dimensionless term (except for spin creepage) defining the deviation of the actual rolling condition between two rigid bodies from pure rolling to rolling coupled with sliding.

In the case of the wheelset running over the rails, creepage is defined in both the longitudinal and the lateral directions and also about the common normal of the contact patch (*spin*) as shown in Fig.2.9 (Dukkipati (2000)). The formulation is provided in Garg and Dukkipati (1984) and Dukkipati (2000) as in Eq.(2.3.a-c).

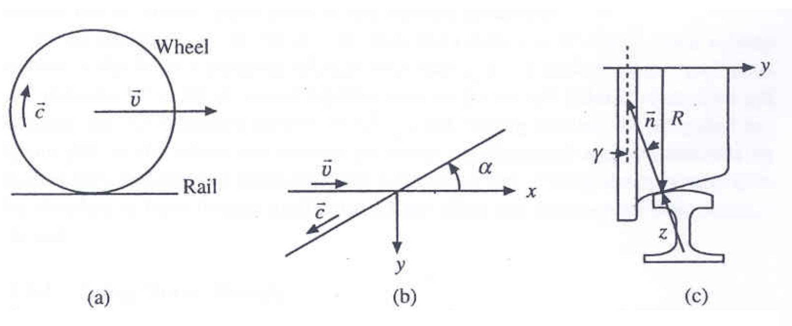

(a) Longitudinal creepage   (b) Lateral creepage   (c) spin creepage

Figure 2.9. Creepage (Dukkipati (2000))

$$\xi_x = \frac{\text{(longitudinal velocity of wheel – longitudinal velocity of rail) at the point of contact}}{\text{Nominal Velocity}} \quad (2.3.a)$$

$$\xi_y = \frac{\text{(lateral velocity of wheel – lateral velocity of rail) at the point of contact}}{\text{Nominal Velocity}} \quad (2.3.b)$$

$$\xi_{sp} = \frac{\text{(angular velocity of wheel – angular velocity of rail) about normal axis at the point of contact}}{\text{Nominal Velocity}} \quad (2.3.c)$$

where ξ_x , ξ_y, ξ_{sp} are the longitudinal, the lateral and the spin creepages respectively. It is important to note that the longitudinal and the lateral creepages are dimensionless, whereas the spin creepage has the dimension of L^{-1}.

2.3.2. The Development of Wheel-Rail Rolling Contact Theory

The wheel-rail rolling contact theory explains the relationship between the creep forces and the creepage. In general wheel-rail rolling contact theory states that there exists a unique relationship between the creepage and the forces generated at the wheel-rail contact patch. These forces are called creep forces as they are generated due to the existence of the creepage.

The relationship between creepage and creep forces was first defined by Carter (1926) who was concerned with the action of locomotive wheels when large tangential forces were transmitted during acceleration and braking. Carter has shown that the difference between the circumferential velocity of a driven wheel and the translational velocity of the wheel over the rail has a non-zero value as soon as a braking or traction couple is applied to the wheel. The difference increases if the braking or traction couple increases, which means that there exists a relationship between the couple and the velocity leading to saturation when the Coulomb friction maximal value is reached. However, the formulation given by Carter was based on solving the integral equation of the two dimensional analysis for a cylinder rolling on a plane which only considers the force on the rolling direction. It is clearly *insufficient* for the purpose of rail wagon/ bogie simulation due to the complex geometries of the wheel and the railhead.

Vermeulen and Johnson (1964) proposed a creep-force law, which included the longitudinal and the lateral creepages. However, the spin creep was left out. To calculate the shape and the size of wheel-rail contact, Hertz theory is used. The Hertz theory defines the contact area between the wheel and the rail as elliptical and the ratio of the semi axes of the ellipse as a function of the curvature of the wheel and the railhead. The treatment of the Hertz theory in detail can be seen in Johnson (1985).

The most successful method of calculating the creep force is presented by Kalker (1967) who then wrote the computer program CONTACT, a universal program for all contact problems of bodies that can be described by half-space. He also has written a program called DUVOROL, which efficiently handles all possible rolling contact problems of bodies with identical elastic constants that touch each other according to the Hertz theory. DUVOROL was used by British Rail to construct a book of tables in support of rail vehicle simulation.

The computational time of both CONTACT and DUVOROL, which are based on Kalker's exact theory, is high and hence they are not suitable for real time applications in vehicle simulation (this is the reason why British Rail constructed a book of tables).

Concerned with this, in 1973 Kalker introduced the simplified theory of rolling contact and then used the theory to build a fast algorithm and computer program FASTSIM (Kalker (1982)).

Shen et al. (1983) improved the Vermeulen and Johnson law by including the effect of spin using Kalker's exact linear theory. The model used by Shen et al. is also called the *heuristic model* and is well known as Shen-Hedrick-Elkins or SHE theory. Fig. 2.10 presents the comparison of the creepage – creep force curve produced using FASTSIM, DUVOROL, and the heuristic model of Shen-Hedrick-Elkins for small spin. The figure shows that the three methods agree very closely.

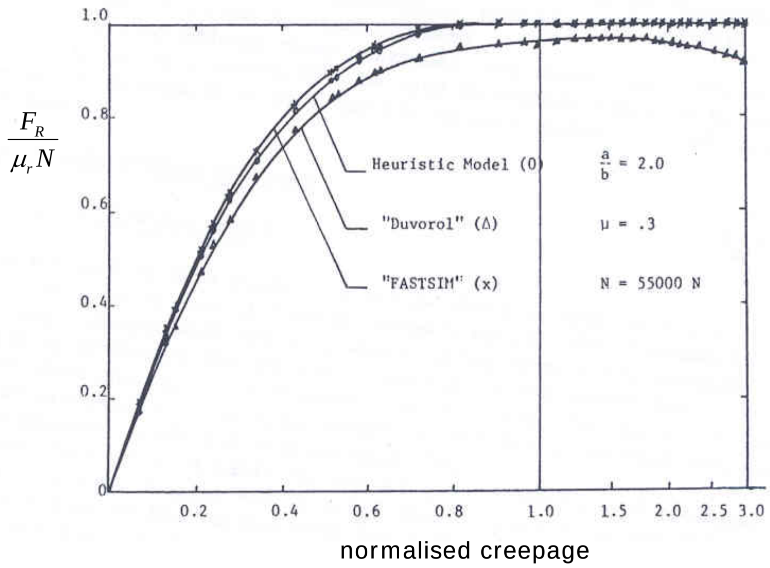

Figure 2.10. Creepage - Creep Force Curves (Shen et al. (1983))

In summary, Kalker (1991) defined the rolling contact theories and their interrelation as shown in Fig 2.11. He also gave a suggestion that the contact mechanics aspect of the wheel and the rail can be treated with the following routines:

Driving/braking wheel action	Shen-Hendrick-Elkins (SHE)
Non flanging vehicle dynamics	BR table book, linear theory, SHE, FASTSIM
Flanging vehicle dynamics	BR table book, FASTSIM
Two-point contact	BR table book, FASTSIM
Wear (profiles)	FASTSIM, CONTACT

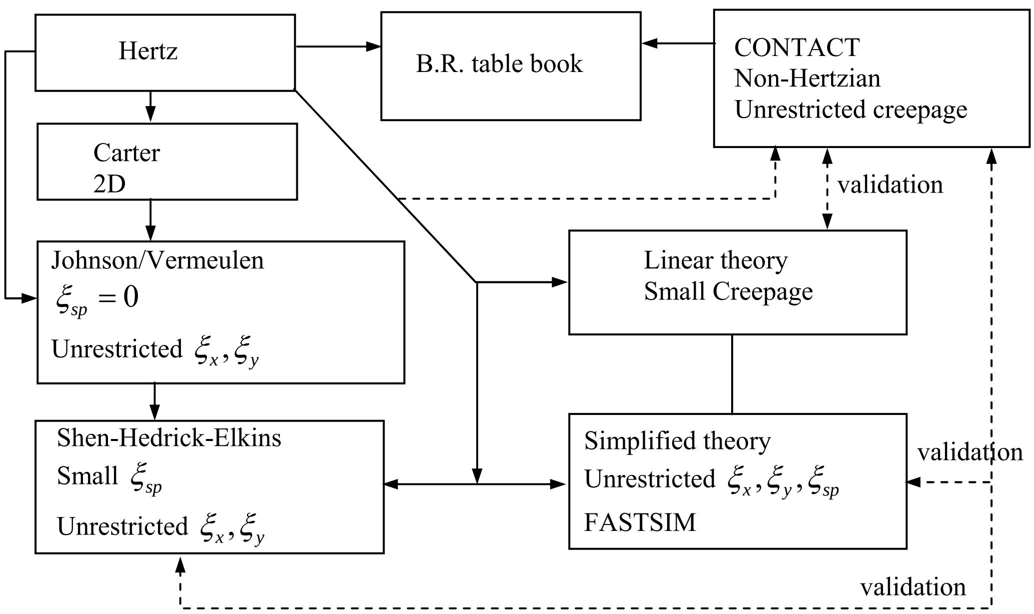

Figure 2.11. Wheel-rail rolling contact theories and their interrelation (Kalker (1991))

To complete our discussion on the development of the wheel-rail rolling contact theory, we should review another method to determine the creep forces which has been recently proposed by Polach (1999). This method is claimed to perform better under high creepage, although it is based on Kalker's work with simplification of the distribution of normal and tangential stresses in the wheel-rail contact patch. According to this theory the creep forces can be computed efficiently with significant saving in computational effort. Application of this method to wagon dynamics simulation was also reported by the author (Polach (2001, 2005)). Polach also extended his creep force model for large creep application by introducing reduction factors for the Kalker coefficient to differentiate the areas of adhesion and slip.

2.4. FREIGHT WAGON BRAKING AND TRACTION SYSTEM

Traction and braking may be regarded as a process of conversion of energy. If a rail wagon is at rest the kinetic energy remains zero, whilst a moving rail wagon possesses significant kinetic energy. Braking reduces the speed of the wagon which means reducing the wagon kinetic energy, whilst traction does the opposite. However, wagons usually do not have their own traction system but are pulled or pushed by locomotives.

Reducing the speed of the wagon requires significant reduction to kinetic energy. The simplest way of reducing the energy is to convert it into heat by contacting material to the rotating wheels or to discs attached to the axles. The material creates friction and converts the kinetic energy into heat energy. With the reduction in kinetic energy, the wagon slows down and when the kinetic energy is fully nullified, the wagon comes to static equilibrium. The vast majority of freight trains are equipped with braking systems that use compressed air as the force to push blocks on to wheels or pads on to discs. These systems are known as "air brakes" or "pneumatic brakes". There are several types of air brake systems that are currently used in trains, which differ in aspects of their control systems, main control equipment, auxiliary equipments and pressure level. This is due to the different standard operating requirements of various railway networks.

Fig 2.12 shows a typical layout of air brake components of a freight wagon (Bureau (2002)) in North America. A similar system is used in the freight wagons of Australia. In this system the compressed air is transmitted along the train through pipes. A control valve, that is the AB type control valve in the figure, controls the pressure level of compressed air used to produce the braking force.

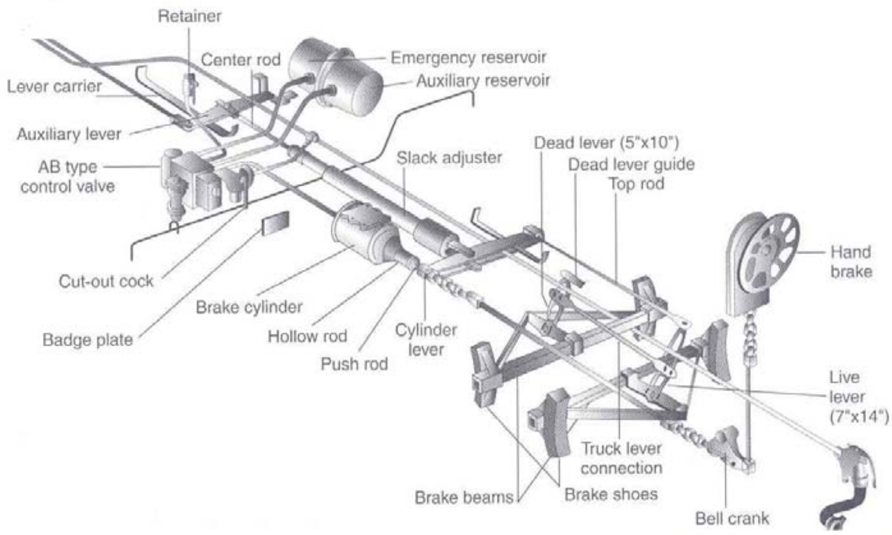

Figure 2.12. Freight wagon air brake system (Bureau (2002))

The braking force produced by the brake cylinder, usually mounted at the wagon underframe, is transmitted through a set of levers and rods to the wagon bogie. The force is then distributed to the wheels through the bogie brake rigging, which consist of levers and brake beams, fitted in each bogie. A slack adjuster is fitted within the mechanical link arrangement. The slack adjuster both takes up and lets out slack in the rods and lever system in order to keep the clearance between the brake shoes and wheels to a specified level.

Fig 2.13 exhibits the typical bogie brake rigging diagram of the three piece bogies that are equipped with one-side push brake shoe arrangement (Handoko et al. (2004)). The link consists of rods and levers suspended from the underframe and bogies, and linked with pins and bushes. The brake rigging requires careful setting up and regular adjustment to ensure the forces are evenly distributed to all wheels.

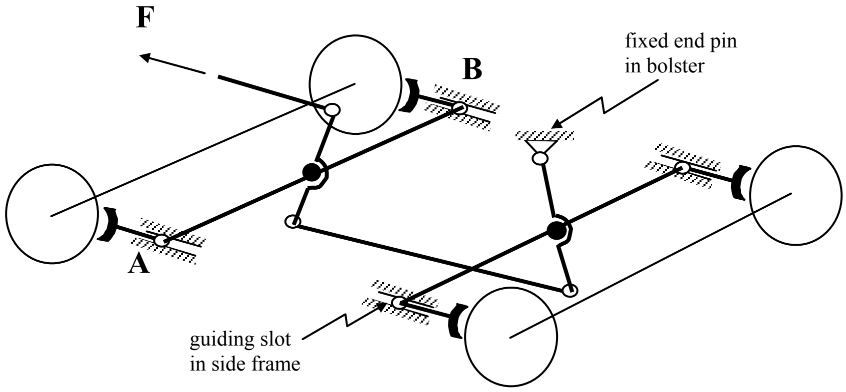

Figure 2.13. Typical bogie brake rigging

It can be seen from the rigging diagram that any bad adjustment of the brake rigging could lead to uneven distribution of braking forces to each wheel. Such a situation can occur when either the centre-pin on rod AB is slightly off-centred or if the fixed-end pin in the bolster is disorientated. The uneven distribution of the braking force to wheels may also occur during curve negotiation if the bogie deforms in shear (warping) mode.

2.4.1. Calculation of Brake Shoe Force

The brake shoe force applied to wheels is calculated from the brake cylinder piston thrust, the total brake rigging ratio (effectively the multiplication factor by which the brake piston force is leveraged by the brake rigging geometry), and the counter-forces exerted by the brake storage spring of the slack adjuster as shown mathematically in Eq. (2.4).

$$F_B = F_{CT}.i_t - (F_R.i_b) \qquad (2.4)$$

where F_B is the brake shoe force, F_{CT} is brake cylinder piston thrust, i_t is total brake rigging ratio, F_R is counter force exerted by slack adjuster, and i_b is the bogie brake rigging ratio. Brake cylinder piston thrust is determined by the cylinder piston area and the pressure in the brake cylinder as shown in Eq.2.5.

$$F_{CT} = \frac{\pi}{4} D^2.p_c \qquad (2.5)$$

where D is effective diameter of the piston and p_c is the air pressure in the brake cylinder. The effective brake shoe force that would be actually acting on the wheel is normally less than the calculated brake shoe force above. This is because of power losses in the rigging system due to friction in the pin joints of the brake rigging levers. If we introduce the brake rigging efficiency η to represent these power losses, then the effective brake shoe force can be written as Eq.2.6.

$$F_{Beff} = F_B.\eta \qquad (2.6)$$

2.4.2. Brake Application and Release Timing

Brake application time is the time required to build the pressure in the brake cylinder and is opposite to the *brake release time,* which is the time required to empty the cylinder. Ideally, the brake is applied simultaneously at the same time on every wagon of a train. This condition is easy to achieve if the electric brake control system is used.

However it will be difficult for the pure pneumatic brake system where the brake command is conveyed through the brake pipe along the train. This is because the response time is limited by the wave propagation in the compressed air system.

For modern freight traffic, it is required to shorten the application and release timing with greater braking force for efficiency of operation. However for the pure pneumatic brake system, problems will arise if the application time is too short because the front end of the train may reach the maximum brake pressure while the rear end would not have reached the full brake pressure yet. Derailments have occurred in which the rear portion of the train "ran into" the front portion in such circumstances. So there should be an optimum brake application time for a given train.

A similar situation (in reverse) happens with the brake release time. The brake will be released if the brake pipe reaches a certain pressure and all the air in the brake cylinder will be exhausted to the atmosphere. Because of the inertia of the air in the pipe system, the brake pipe pressure in the wagon near to the locomotive, from where the compressed air is supplied, may have reached the required pressure while the rear end would not have yet.

Due to the reasons explained above and also to assure the compatibility among brake systems in use, the UIC, BS, AAR, and other main railway standards have limited the brake application and release times to certain values. This limitation is prescribed for safety reasoning and decided based on experience. For example, the UIC standard prescribes the brake application and release timing for freight cars fitted with single pipe gradual release of brake as follows:

Application time : 0 to 95 % max brake cylinder pressure is 18 sec to 30 sec

Release time : 0 to 95 % max brake cylinder pressure is 45sec to 60 sec

From the application time and release time we can clearly see that, during the braking process, the force applied to the wheel will not be constant; rather it will build up slowly from zero to maximum. This also means that the wagon deceleration will change with time.

2.4.3. Traction

Traction, in general, can be viewed as the reverse process of braking. From this point of view, all parameters that influence the dynamics of wagons during braking can also affect the dynamics of wagons during traction. However, most of the freight wagons are not self-propelled. To accelerate they get the pulling or pushing force from a locomotive. The traction forces in a locomotive are usually generated by diesel engine or electric traction motors that produce torque transmitted to the wheelset using a gear box, whilst the wagons receive the traction force through pulling or pushing action of the mechanical couplers.

2.5. LONGITUDINAL DYNAMICS OF BOGIES AND WAGONS

2.5.1. Basic Principle of Braking Dynamics

During braking, forces or torques are applied to the wheelsets in order to decelerate the wagon. This process also produces reaction force in couplers and pitch torque to the wagon body and bogie. These forces affect the running stability and curving performance of bogies and wagons. On the other hand the dynamic response of the wagon such as the change of the load distribution to the wheel can also affect the braking performance. The braking performance is usually measured through the stopping distance and also from the occurrence of skidding or wheelslide. With the reduction of the wheel load, the chance of the skid occurrence increases. Braking also involves friction, a complex phenomenon. During the process of braking, friction occurs between the brake shoe and the wheel and between the wheel and the rail as shown in Fig. 2.14.

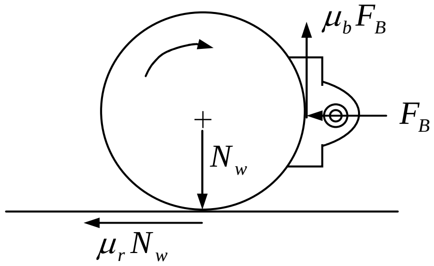

Figure 2.14. Forces at the braked wheel

The brake shoe force applied to the wheel F_B produces tangential force $\mu_b F_B$. If the wheel has radius r_w, a braking torque T_B is generated as shown in Eq.2.7.

$$T_B = \mu_b F_B r_w \qquad (2.7)$$

The free body diagram of the braked wheel shown in Fig. 2.15 represents a wheel moving longitudinally in the x-direction at speed V and with angular velocity ω. J_y, r_w and T_B denote the polar moment of inertia, wheel radius and brake torque respectively. At the contact point between the wheel and the rail, longitudinal and vertical forces F_x and F_Z respectively arise as the reaction to the brake torque and the static weight mg.

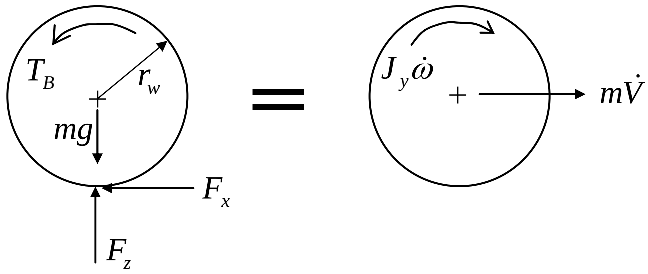

Figure 2.15. Free body diagram of braked wheel

By balancing the forces in the x- and z- directions and moments about the centre of mass of the wheel, three scalar equations of a braked wheel are established:

$$\left.\begin{aligned} m\dot{V} &= -F_x \\ F_z &= mg \\ J_y\dot{\omega} &= F_x r_w - T_B \end{aligned}\right\} \qquad (2.8)$$

where m is the mass of the wheel and wagon supported by the wheel and g is the gravity constant, while over dots denote differentiation with respect to time.

2.5.2. Skid and Friction Coefficient

Severe braking force can cause the wheelset to get locked and slide on the rail. This phenomenon is called skidding. This could lead to geometry damage to the wheels (wheel flat) and the railhead. Skidding also makes the stopping distance longer that would be dangerous to the train operation. Hence skidding should be avoided during braking as a matter of priority.

Skidding occurs when the braking force exceeds the adherence offered by the wheel-rail contact patch. Thus, to avoid skidding of the wheels during brake application the brake force at the brake shoe must invariably be kept lower than the adhesion at the rail. Skidding does not occur when the relationship in Eq. (2.9) is fulfilled.

$$\mu_b F_B < \mu_r N_W \tag{2.9}$$

Currently many rail wagons are equipped with equipment to prevent skidding. However, there are still many wagons that do not possess this equipment, especially freight wagons, due to costs.

The difficulty in controlling skidding is related to the friction characteristic between materials that vary in nature. For example, friction between the wheel and the rail varies with rail surface condition (Macfarlane (2000)) such as rail corrugations, rail head contamination from oily deposits, leaves, water, ice, sand, etc, and the wheel tread surface condition as the application of the different type of brake shoe on the car (iron block, composition block, disc). Friction between the wheel and the rail also varies with the position of the wheelset along the track. The leading wheelset usually encounters the dirtiest rail and worst adhesion condition, and then cleans it for the wheels that follow. For design purpose, the friction coefficient between the wheel and the rail is usually assumed to be between 0.10 - 0.30.

In Section 2.3, the relation between creepage and the generated creep force has been explained. However, many experiments reported in the literature show that the relation has a peak followed by decay with increase in creepage. To explain this phenomenon, Nielsen and Theiler (1996) proposed the modelling of the friction coefficient as a function of slip velocity. Following the theory of Nielsen and Theiler, the relation between the slip percentage and the friction between wheel and rail was proposed by Ohishi et al. (2000), as exhibited in the adhesion force versus slip velocity curve shown in Fig.2.16. Because the adhesion forces depend only on the friction coefficient and normal load, it is clear that the friction coefficient is also affected by the slip. The relation between them is not linear and depends on the wheel/rail condition (wet or dry).

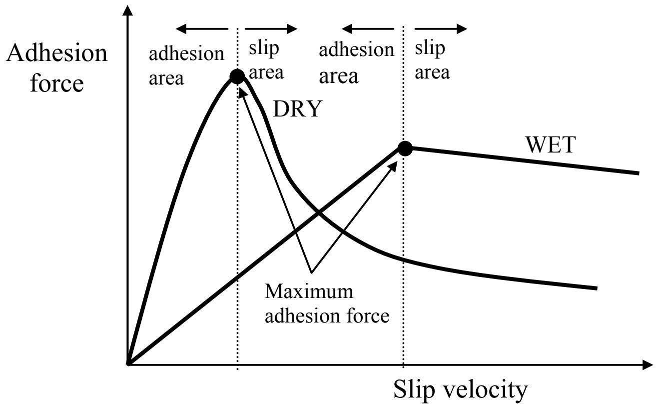

Figure 2.16. Adhesion force against slip velocity (Ohishi et al. (2000))

Coefficient of friction between the brake shoes and the wheel also does not remain constant. It varies with the sliding speed between the brake shoes and the wheal tread that depends on the velocity of the wagons. This also means that it changes continuously during the braking process. Fig 2.17 exhibits a typical plot of kinetic friction coefficient between two surfaces as a function of sliding speed and the Barwel's formula that shows the relationship between the friction coefficient μ_k and sliding speed v_s where the constant c_f depends on the material (Rabinowicz (1995)).

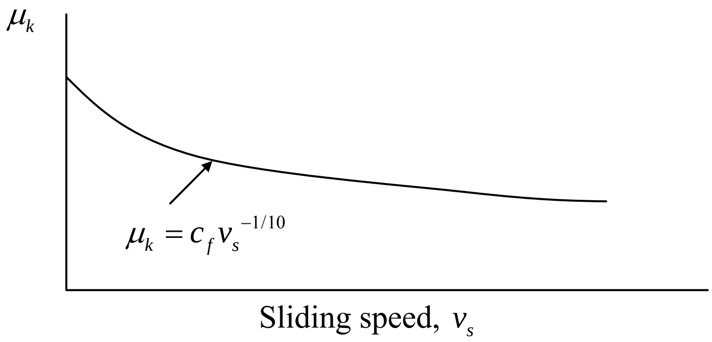

Figure 2.17. Friction coefficient against sliding speed

2.5.3. Dynamics Due to Traction

Because traction can be viewed as the reverse process of braking, the three scalar equations in the Eq. (2.8) are still applicable with only a change of sign (+/-). As a consequence, in the reverse of the skid phenomenon during braking, locomotives exerting excessive traction torque can make the wheelset rotate without any longitudinal motion. This condition is referred to as 'roll-slip' and becomes a subject of interest in the locomotive drive simulation as reported by Muller and Kogel (2000). Roll-slip can lead to railhead damage (engine burn or wheel burn). As for braking, traction can also cause large longitudinal forces in the wheel-rail contact patch.

2.5.4. State-of-the-art of Braking and Traction Dynamics Research

Balas (2001) developed a model for the sliding wheel of a railway car during braking. This work is mainly to assist the study and design of the braking equipment, including the Anti-lock Braking System (ABS). In this model the friction coefficient between the wheel and the rail is considered as a function of the slip of the wheel as shown in Fig 2.18. The slip of the wheel is defined as shown in Eq.2.10.

$$s = (v_{car} - v_w) / v_{car} \tag{2.10}$$

where: s is the slip (always between 0 (no braking) and 1 (locking)), v_{car} is the velocity of the car and v_w is the velocity of the wheel. This concept has been used by Ohishi et al. (2000) to design a control system that would prevent slip during traction of an electric motor coach. The difference is only in the shape of the friction coefficient against slip curve where Balas considers the pseudo sliding due to elasticity of the wheel. If this pseudo sliding is ignored, then the curve in Fig.2.16 used by Ohishi will be obtained.

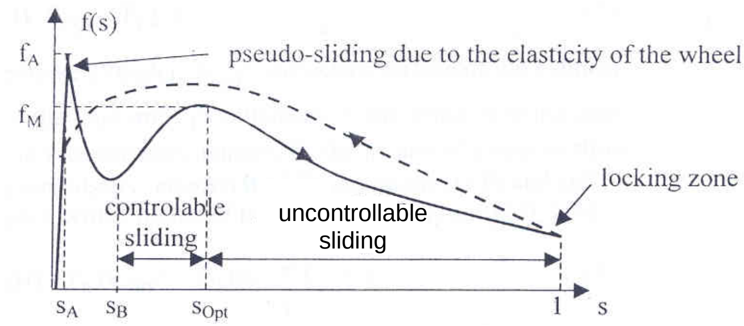

Figure 2.18. Wheel-rail friction coefficient against slip (Balas (2001))

Independently Cocci et al. (2001) presented a railway wagon model with an anti-slip braking system. The model is set up in the ADAMS/Rail and Simulink platform. Similar to Balas, Cocci et al. also considered the friction coefficient between wheel and rail as a function of wheel slip. The bogie suspension is modelled in three dimensions where longitudinal, vertical, and lateral stiffness are considered in the model. However longitudinal dynamics due to the effect of anti-slip control for optimum deceleration was particularly attended. Modelling the complete bogie is required to take into account the effect of load distribution to the wheel due to track geometry and/or track irregularities.

Olson (2001) has studied the longitudinal dynamics of ground vehicles that include non-linear wheel braking and acceleration models. Although his work is focused on road vehicles, it is still appropriate to the study of railway wagon braking. In formulating the equations of motion of wheel under braking condition, Olson considered the slip as a dynamic state variable, replacing the absolute rotational rate of the wheel speed.

Lixin and Haitao (2001) studied the dynamic response of wagons in a heavy haul train during braking mode. For such purpose they have set up a model using ADAMS/Rail software that could predict the three dimensional dynamic response of the wagon under braking conditions. An open-top freight wagon used in China was the case study. From their investigation it was concluded that the application of braking has adversely affected the lateral and vertical dynamic performance of the wagon. However, the investigation was limited to constant brake shoe force that was distributed evenly to the wheels. In actual conditions, the brake force is a time function and may not be symmetric and could be distributed unevenly to the wheels. Lixin and Haitao (2001) *did not* investigate the effect of wheel-lock or skid phenomena. Both of these conditions (asymmetric brake forces and wheel skid) can lead to a more serious situation. This thesis (Chapter 9) describes these phenomena in detail.

Berghuvud (2002) investigated the effect of brake application to wagon curving performance using parameters that define the wagon curving performance such as the wheelset angle of attack, the track forces, and the wear in the contact patch between the wheels and the rails. He found that the wagons with different types of bogies respond in different ways to curving as a function of the applied braking force. However he *did not* consider the effect of variation in speed or deceleration as he examined the wagon running on downhill slopes while braking was continuously applied to keep its speed constant. The braking force applied also remained constant and symmetric with no wheel skid.

Suda and Grencik (1996) explained the mechanism of deterioration of curving performance under braking conditions where the braking torque reduced the steering torque of the wheelset. This mechanism is explained in Fig.2.19 that shows a free body diagram of a wheelset running along a curved track.

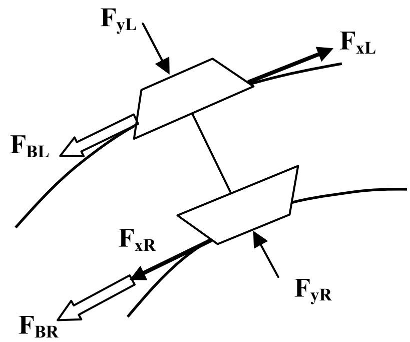

Figure 2.19. Curving diagram of a wheelset (Suda and Grencik (1996))

While negotiating a curve, the rolling radius of the outer wheel becomes larger than that of the inner wheel leading to the generation of longitudinal creep forces F_{xR} and F_{xL}, where in general $F_{xR} \neq F_{xL}$. These creep forces produce a steering torque that guides the wheelset to follow the curve appropriately. Application of brake produces additional longitudinal forces F_{BR} and F_{BL} on the contact points which produce a steering moment as shown in Eq.(2.11).

$$M = a\left[\left(F_{xL} - F_{BL}\right) + \left(F_{xR} + F_{BR}\right)\right], \tag{2.11}$$

where a is the semi distance between the contact points. However, the resultant of total longitudinal creep force and lateral creep force at the contact points cannot exceed the maximum frictional force between the wheel and the rail. The resultant creep forces are calculated as shown in Eq.(2.12).

$$F_{CR}=\sqrt{\left(F_{xR}+F_{BR}\right)^2+F_{yR}^{\ 2}} \quad ; \; F_{CL}=\sqrt{\left(F_{xL}-F_{BL}\right)^2+F_{yL}^{\ 2}} \tag{2.12}$$

where F_{CR} and F_{CL} are resultant creep forces on the right and left rail respectively. If F_{CR} and F_{CL} exceed the creep condition, they becomes saturated leading to reduction in the longitudinal creep force. The directions of longitudinal creep force and additional force due to braking are the same on the inner wheel, so the reduction in longitudinal force on the inner rail is larger than that on the outer wheel. Because of this reduction of longitudinal forces, the steering moment on the wheelset also reduces.

Malvezzi et al. (2003) carried out an investigation of the braking in trains. They performed probability analysis of train deceleration during braking. The aim of the work was to determine the probability that the real deceleration is lower than the nominal value multiplied by a safety margin.

The analysis of braking in a train was also carried out by Durali and Shadmehri (2003). The authors reported the analysis of train derailment due to severe braking with various wagon weight configurations. From the results, the optimum configuration of wagons and the critical derailment velocity can be determined. The authors also claimed that the results were in excellent agreement with the field experience although they did not present any comparison with the field data in the paper.

Excessive traction torque applied to the locomotive wheels could cause roll-slip. Because this roll-slip reduces the traction power and can damage the locomotive's wheels, it is very important to avoid it during the operation of the motive power. For this reason, studies on the subject of slip controllers have been extensively performed. Among them was the work recently reported by Frylmark and Johnsson (2003). In their thesis Frylmark and Johnsson studied several methods of slip controller such as adhesion observer based controller, fuzzy logic slip controller and hybrid slip control method. As a summary, the authors presented the advantages and disadvantages of each method. They also proposed a few improvements and present ideas that may be interesting in future research.

2.6. WAGON SIMULATION SOFTWARE PACKAGES

The computational simulation of the dynamic behaviour of railway wagons has been a standard design task in the railway industry during recent years (Schupp (2003)). Software packages such as VAMPIRE and NUCARS (Iwnicky (1999)) have been specifically developed for this purpose, while general multibody dynamics software tools such as and ADAMS, SIMPACK and UNIVERSAL MECHANISM have a module which is intended to simulate the railway wagon dynamics. Multibody dynamics computational method has been used as a tool to develop these software packages.

Using VAMPIRE as a tool, McClanachan et al. (2004) have shown that it is possible to adequately model freight wagons containing three piece bogies during constant speed operation. In their paper, the data from field tests were compared with the simulation of roll, bounce and pitch.

Shabana and Sany (2001) reported a survey of rail vehicle track simulations which include flexible multibody dynamics. In their paper they have pointed out that, with the recent development in computational mechanics, it is possible to develop a tool to comprehensively analyse the complex dynamics of railway vehicles and tracks.

Shen and Pratt (2001) developed a railway dynamics modelling and simulation package for current industrial trends. They suggested that the future software tool should adopt the object oriented and knowledge based techniques that aid the human thought process. According to them the new simulation packages should be adaptable to design changes.

2.6.1. Reference Coordinate System and Formulation of Equation of Motion

This section discusses how the multibody system approach is currently used in the formulation of railway vehicle dynamics simulation tools. The review includes the equation of motion and the formulation of the wheel-rail contact problem. These are the specific modelling features that make the railway vehicle dynamic simulation unique. However the review presented here also shows that the current approach is not ideal to simulate railway wagon/ bogie dynamics during braking or traction.

The common method of deriving the equations of motion of the railway wagon is the transfer coordinate (or moving coordinate) system that moves along the track at the speed of the wagon. This coordinate system is referred to as track-based or track-following moving reference system (Zboinski (1999)). With this method it is very convenient to describe the position of the contact point between the wheel and the rail and the direction of wheel-rail contact force. By assuming steady state motion of wagons, a simple form of the equations of motion can be obtained. However, applying this method to the braking and/ or traction condition is rather cumbersome if not impossible.

Fig 2.20 illustrated this problem where a body i, with body coordinate system ($o_i, \mathbf{x}_i, \mathbf{y}_i, \mathbf{z}_i$) attached to it, is moving with respect to a non-inertial transfer coordinate reference system R ($o_r, \mathbf{x}_r, \mathbf{y}_r, \mathbf{z}_r$). As presented by Schiehlen (1984) and Xia (2002), the Newton-Euler equations of motion for the moving body i with respect to the transfer coordinate system and the inertial reference frame O ($o_o, \mathbf{x}_o, \mathbf{y}_o, \mathbf{z}_o$) are as per detail shown in Eq.(2.13) and Eq.(2.14).

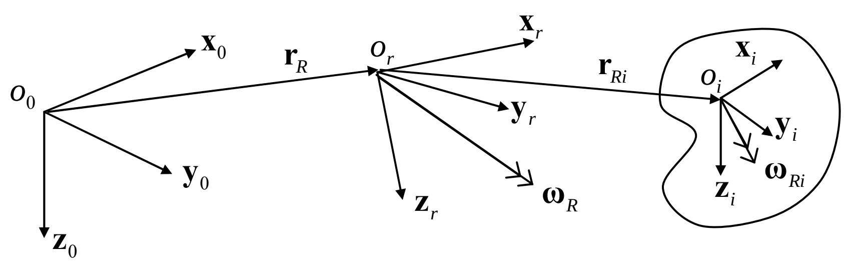

Figure 2.20. The description of the motion of a body in a moving reference frame

$$\mathbf{m}_i\left[\ddot{\mathbf{r}}_R + \tilde{\boldsymbol{\omega}}_R\dot{\mathbf{r}}_R + \left(\dot{\tilde{\boldsymbol{\omega}}}_R + \tilde{\boldsymbol{\omega}}_R^2\right)\mathbf{r}_{Ri} + 2\tilde{\boldsymbol{\omega}}_R\dot{\mathbf{r}}_{Ri} + \ddot{\mathbf{r}}_{Ri}\right] = \mathbf{F}_i \tag{2.13}$$

$$\mathbf{I}_i\dot{\boldsymbol{\omega}}_R + \tilde{\boldsymbol{\omega}}_R\mathbf{I}_i\boldsymbol{\omega}_R + \tilde{\boldsymbol{\omega}}_R\boldsymbol{\omega}_{Ri}(\mathbf{I}_{xi} + \mathbf{I}_{yi} + \mathbf{I}_{zi}) + 2\tilde{\boldsymbol{\omega}}_{Ri}\mathbf{I}_i\boldsymbol{\omega}_R + \mathbf{I}_i\dot{\boldsymbol{\omega}}_{Ri} + \tilde{\boldsymbol{\omega}}_{Ri}\mathbf{I}_i\boldsymbol{\omega}_{Ri} = \mathbf{M}_i \tag{2.14}$$

where $\mathbf{m}_i$ and $\mathbf{I}_i$ are the mass matrix and the inertia tensor of the body respectively, $\mathbf{F}_i$ and $\mathbf{M}_i$ are the external force and moment applied to the body written in the transfer coordinate frame respectively, $\mathbf{r}_R$ and $\boldsymbol{\omega}_R$ are the vector position and the angular velocity of the transfer coordinate system respectively, and $\mathbf{r}_{Ri}$ and $\boldsymbol{\omega}_{Ri}$ are the vector position and angular velocity of the body reference in respect to the transfer coordinate system respectively. Over dots ($\dot{}$) represent differentiation with respect to time and tildes (~) represent skew symmetric matrix of the vector.

If the transfer coordinate system moves with constant speed along a tangent track, then the Newton-Euler equations of motion reduce to a very simple form as shown in Eq.2.15 and Eq.2.16.

$$\mathbf{m}_i \ddot{\mathbf{r}}_{Ri} = \mathbf{F}_i \tag{2.15}$$

$$\mathbf{I}_i \dot{\boldsymbol{\omega}}_{Ri} + \tilde{\boldsymbol{\omega}}_{Ri} \mathbf{I}_i \boldsymbol{\omega}_{Ri} = \mathbf{M}_i \tag{2.16}$$

The equations will be slightly more complex if the system moves in curving, although it can be handled without much difficulty as long as the speed remains constant because we could pre-define the angular velocity of the transfer coordinate system for the known geometry of the curve.

The problem becomes very complex when we deal with the braking condition where the speed does not remain constant. Currently, the solution to this problem is obtained by pre-guessing the speed profile based on the initial velocity and deceleration and *assuming* the transfer coordinate system to move with this speed profile. This approach *will not provide* an exact solution because the deceleration actually comes from the force applied to the body in the system, or more specifically it is caused by the force generated at the contact points due to brake forces applied to the wheels. To obtain an exact solution, the contact kinematics should be calculated as a function of the variation of the velocity of the moving body and it must be calculated in real time (on line) during the simulation.

Another consequence of using a moving reference frame is that the wheelset rotation with respect to its lateral axis, which is referred to as *wheelset pitch*, is not explicitly included in the formulation. Because the speed of the wagon has been pre-defined and assumed to be the speed of the transfer coordinate system along the track, the nominal wheelset pitch velocity has also to be pre-defined as a function of the speed. Thus, the effect of the severe application of heavy braking and traction such as skid and slip *cannot* be accounted for in the formulation.

Due to the reasons explained above, the best way to treat the dynamics during braking and traction is to describe the absolute body motion in the *fixed inertia coordinate system*. This thesis presents such a formulation which is discussed in Chapter 3.

Another matter that should receive careful attention is the interaction between the wheel and the rail itself. Under braking torque, the locked region in the wheel-rail contact area is moved backward and generates areas of compression and tension as shown in Fig 2.21 (Dukkipati (2000)). In parallel, the forward motion of the wagon is decelerated by the longitudinal creep force developed in the contact area. The larger the longitudinal creep force, the further the zero line of stress is displaced from a line drawn perpendicular to the rail and through the centre of the wheel. If the longitudinal creep force is large enough, all the contact area becomes a slip area or in other words the wheel will purely slide (skid) on the rail. Skidding affects the safety of the wagon so it is important to consider it in the wheelset dynamic model. The problem will be more complicated if the friction coefficients between the wheel and the rail and between the brake shoe and the wheel are treated as dynamic variables.

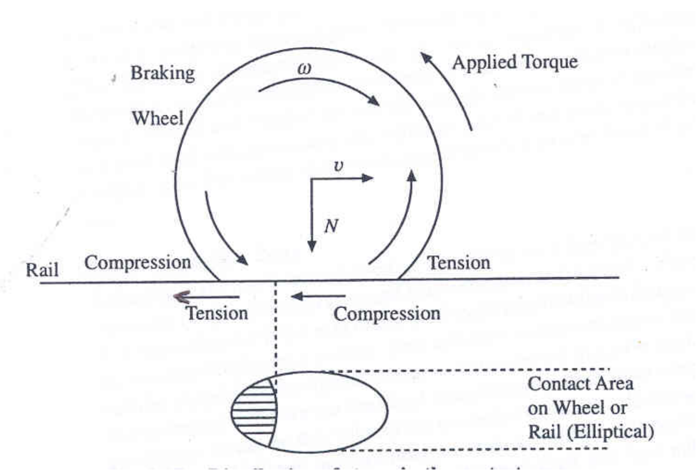

Figure 2.21. Stress distribution in the contact area during braking (Dukkipati (2000))

We should also note that the magnitude of the total creep force is limited by the saturation adhesive force between the wheel and the rail. As the total creep force is the resultant of the longitudinal and lateral creep forces, we can deduce that at saturation the longitudinal creep force could effectively modify the lateral and roll motions between the wheel and the rail. From this fact we can also state that the application of the braking force affects the lateral as well as the longitudinal and the vertical dynamics of the wagon, especially at the onset of and during skidding.

2.7. SUMMARY

Railway wagon, bogie and wheelset dynamics cover the subjects of linear and non-linear stability, curving performance, ride quality and comfort analysis, wagon track interaction, and dynamic control systems. This extensive research is greatly supported by the emergence of wheel-rail rolling contact theory and the improvement of numerical analysis algorithms and computational strategies over the last three decades.

Only limited information on the dynamic behaviour of wagons and bogies under longitudinal forces due to braking and traction are found in the published literature. As wagons are mostly not self-propelled, the interest in the research of the effect of longitudinal forces due to braking is much larger. Much of the research on wagon braking is concerned only with the optimisation of braking distance and to avoid wheel skid. At the onset of and during skidding, the longitudinal creep force affects the lateral creep force at the wheel-rail contact patch as the magnitude of the resultant of the lateral and longitudinal creep force is limited by the saturation adhesive force between the wheel and the rail. The effect of the braking force to the lateral dynamics of the wagon bogie especially at the onset of and during skidding is addressed in this thesis.

The complexity of modelling the dynamics of bogies during traction/braking emerges as we cannot use a transfer coordinate system that moves along the track at the speed of the wagon. The position and orientation of the contact patch, the creepages and creep forces, which are usually defined in the track reference frame, need to be transferred to the absolute reference frame to formulate the equations of motions. A comprehensive explanation of the dynamic behaviour of the bogie under traction/braking condition is undoubtedly required to maximise the efficiency and minimise the risk of railway rollingstock operation. This thesis provides a contribution to this important area.